Supporting Information

- Ni-Zn-B MAB phases Synthesis:

Since Ni melts at 1455 °C, boron melts at 2095 °C and zinc has a melting point of 420 °C, the synthesis of Ni-Zn-B MAB phases, Ni_2ZnB and Ni_3ZnB_2, is intriguing. Moreover, zinc boils at 907 °C which means that going through regular solidification synthesis, will lead to evaporation of zinc before melting the other elements. Using excess zinc, also known as the metal flux method, is also not the proper method to synthesize these MAB phases since Zn is involved in the reaction and the possibility of side reactions is very high. Based on the Ni-B binary phase diagram, Ni_2B forms congruently and has a melting point of 1125 °C which is much lower than that of Ni and B in their elemental forms. Thus, Ni_2B was selected as a master alloy in order to provide nickel and boron for the synthesis. A properly mixed nickel (Arcos Organic-99.9%) and boron (Alfa aesar-99%) powder, which was cold-pressed into a pellet, was arc melted in an inert atmosphere as explained previously (1). The synthesized master alloy button was flipped and re-melted to provide better homogeneity, leading to a single-phase synthesis as confirmed by its X-ray diffraction pattern (**Figure S2**). In the next step, the powdered master alloy was mixed with proper amounts of zinc (Alfa Aesar 97%) and nickel powder (Arcos Organic-99.9%), pressed into a pellet and sealed in a quartz tube under vacuum, after purging the tube with argon multiple times. Then the sample was pre-alloyed at 700 °C for 36 hours. The pre-alloyed samples were then crushed, mixed, pressed and submitted to the temperature-time profiles shown in **Figure S3**.

- Etching process:

All the MXene phases including Ti_3AlC_2 , as the first and most studied one, have been etched via HF (2) or HCl-LiF (3). Although HF is the most efficient acid for MXene etching, it was shown to be ineffective for etching MAB phases. (4) In fact, A is notably more difficult to etch out of MAB phases than in MAX phases, more aggressive etchants (NaOH, HCl) have been used in the literature for etching MAB phases.

We have therefore tested 1M HCl and 0.5 M NaOH, as well as another etchant, $FeCl_3$/HCl (5g $FeCl_3$ dissolved in 100 mL 10% HCl), used for etching Zn in metallurgical processes. The same etching temperature and time (room temperature, 72 h) were used in all cases: HCl showed the most promising results. According to XRD data no etching occurred upon treatment with $FeCl_3$/HCl and NaOH.

According to preliminary analyses, the zinc interlayer was only partially etched via exposing the synthesized powder to 1 M HCl solution in a beaker with regular ultrasonication to accelerate the etching process. During etching, hydrogen bubbles evolved proving that etching occurred. However, most of the sample (unetched) remained at the bottom of the beaker and only a small number of partially etched particles floated on the liquid' surface or were suspended in solution (details to be communicated elsewhere). The larger unetched bottom particles, which are the focus of this study, were collected and washed for further investigations and these.

- X-Ray diffraction analysis:

In order to confirm the synthesis, the alloy was investigated via powder X-ray diffraction (PXRD). Phase analysis was performed by X-ray powder diffraction at room temperature with a Rigaku MiniFlex 600, using a Cu Kα radiation source (λ=1.5418 Å). Rietveld refinement (full-matrix least-squares refinement) was performed using the FULLPROF program(5).

- ICP analysis:

Inductively coupled plasma (ICP) analysis was carried out on the etched and unetched MAB phases. All the measurements were done on a Perkin-Elmer Optima 7300DV apparatus in the Environmental Science Research Laboratory at the University of California, Riverside.

Although the morphology of the particles changed after etching, the composition of the MAB phases did not change significantly. It was observed that the Ni:Zn ratio changes from 2.20 to 2.15 and from 3.16 to 3.13 respectively for Ni_2ZnB and Ni_3ZnB_2. This slight changes in compositions after etching were accompanied by the creation of pores (Ni_2ZnB) or sheet openings (Ni_3ZnB_2) in these MAB phases as demonstrated by HRSEM images. Although the XRD showed a clean synthesis for both phases, small Ni-rich regions and cracks were detected in the backscattering microstructure imaging of polished bulk Ni_2ZnB samples (**Figure S6**). These Ni-rich regions and the cracks already in the microstructure may have assisted the pore generation, as shown by the enlargement of pores of a fractured surface of Ni_2ZnB submitted to an acid bath for 5 hours (**Figure S8**). In Ni_3ZnB_2, the sample showed less Ni rich regions and cracks in the microstructure, making it more stable in acid.

- **Electrochemical Analyses:**

Battery electrochemical analyses were performed with two-electrode 2032-type coin cells. In the half cells to test the Ni_2ZnB materials, the working electrode was composed of 80 wt.% of Ni_2ZnB, 10 wt.% of polyvinylidene difluoride (PVDF) as binder, and 10 wt.% of acetylene black and cast on copper foil. The typical areal loading was ~ 2 mg cm^{-2}. The electrolyte was composed of Lithium hexafluorophosphate ($LiPF_6$) solution (1 M) in a mixture of ethylene carbonate (EC) and diethyl carbonate (DEC) (volume ratio EC: DEC= 50:50). Commercial lithium foil (750 μm thickness) is used as the counter electrode. Galvanostatic cycling was performed between 0.01 and 3.0 V vs Li/Li^+ in half cells. The current densities for Ni_2ZnB electrode were 20, 100 and 300 mA g^{-1}. Cyclic voltammetry was performed using scan rates of 0.1 mV s^{-1} between 0.01 and 3.0 V vs Li/Li^+. The above procedures were the same for Ni_3ZnB_2.

- **SEM and TEM Analyses:**

The surface morphology and elemental mapping of the synthesized materials were investigated by scanning electron microscopy (SEM) and energy dispersive X-ray spectroscopy (EDS), respectively, on an ultra-high-resolution low-energy system Nova NanoSEM450 equipped with a 50 mm^2 X-Max50 SD EDX detector. The thin samples for transmission electron microscopy (TEM) were deposited on a copper holey carbon grid and analyzed using a ThermoFisher Scientific (formerly FEI/Philips) Titan Themis 300 instrument. After washing and sonication for few minutes in distilled water, the layers were scooped from the liquid via the grids for TEM investigations. Both instruments are located at the center facility for advanced microscopy and microanalysis (CFAMM) of the University of California, Riverside.

- **X-ray photoelectron spectroscopy (XPS)**

X-ray photoelectron spectroscopy (XPS) data was collected on a Kratos AXIS Supra (Al Kα=1486.7 eV) instrument at UC Irvine Materials Research Institute (IMRI). The coin cells were disassembled in the argon filled glove box for preparing the sample for XPS analysis. Electrodes were washed by dimethyl carbonate and then dried under vacuum at 60℃ inside a glovebox. After that, the prepared samples were stored in a stainless-steel tube with KF flange sealing. Then the samples were transferred to a glove box integrated to the Kratos AXIS Supra instrument for further XPS analysis. The reference peak of C 1s at 284.6 eV were used to calibrate the XPS data.

Figures:

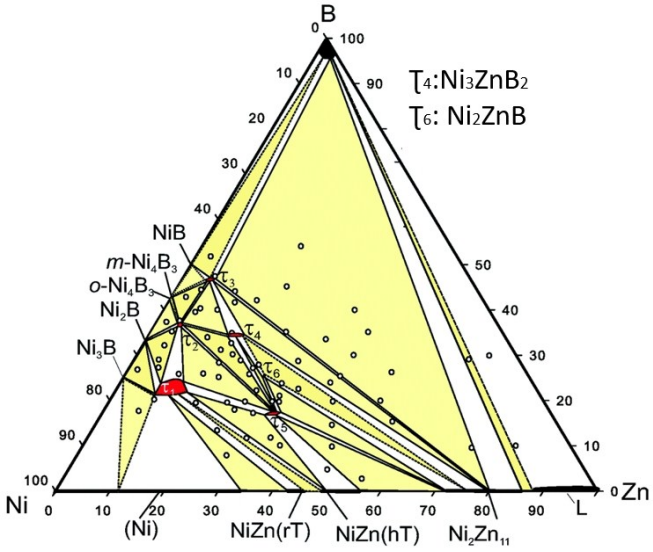

Figure S1. Ni-Zn-B ternary isotherm at 800°C. Reproduced from reference (6).

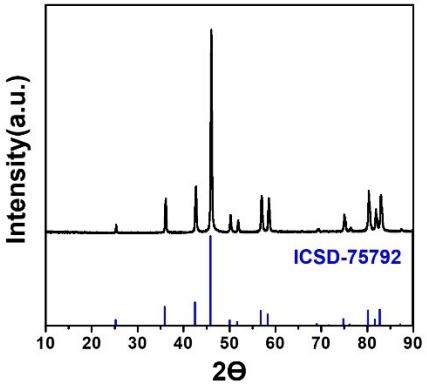

Figure S2. Powder XRD analysis of Ni_2B master alloy arc-melted prior to MAB Synthesis

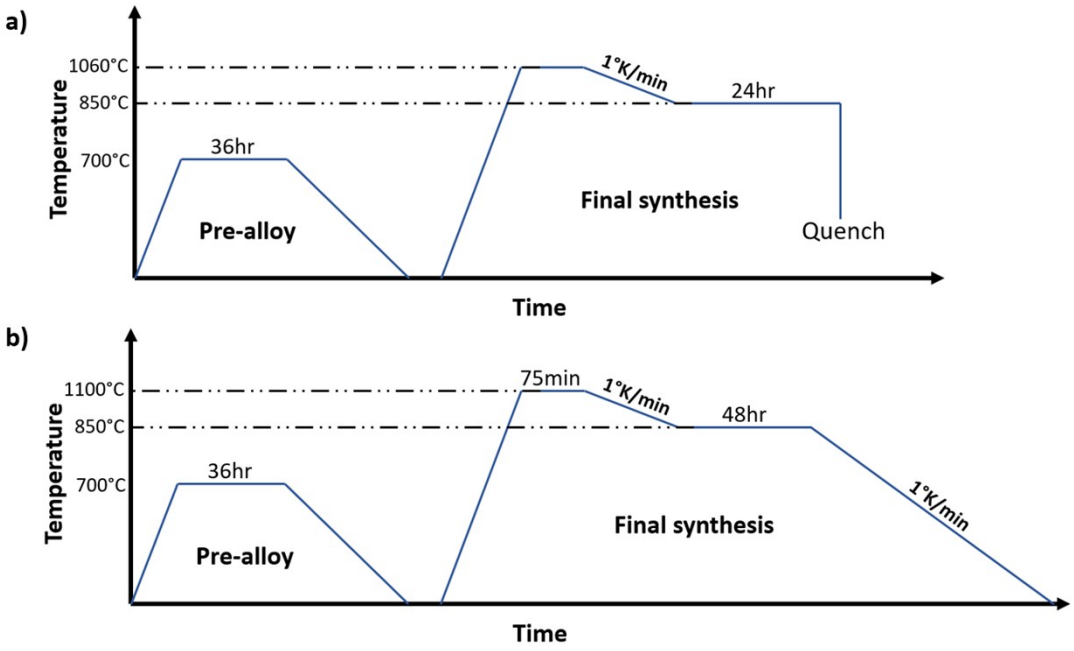

Figure S3. Temperature-time synthesis profile of (a) Ni_2ZnB and (b)Ni_3ZnB_2

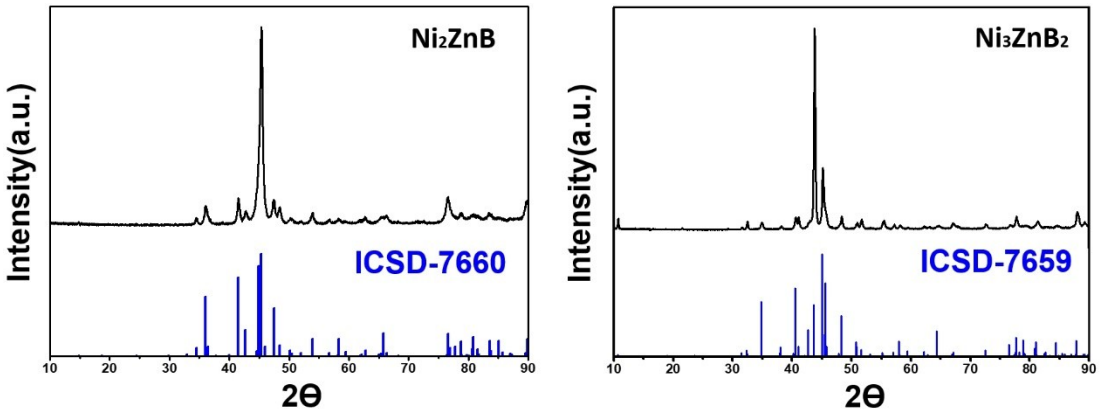

Figure S4. Powder XRD analysis of (a) Ni_2ZnB and (b) Ni_3ZnB_2 showing intensity mishmashes when compared with theoretical patterns (blue), indicating preferred orientation (sheets morphology, **cf. Figure S6**) of the crystallites.

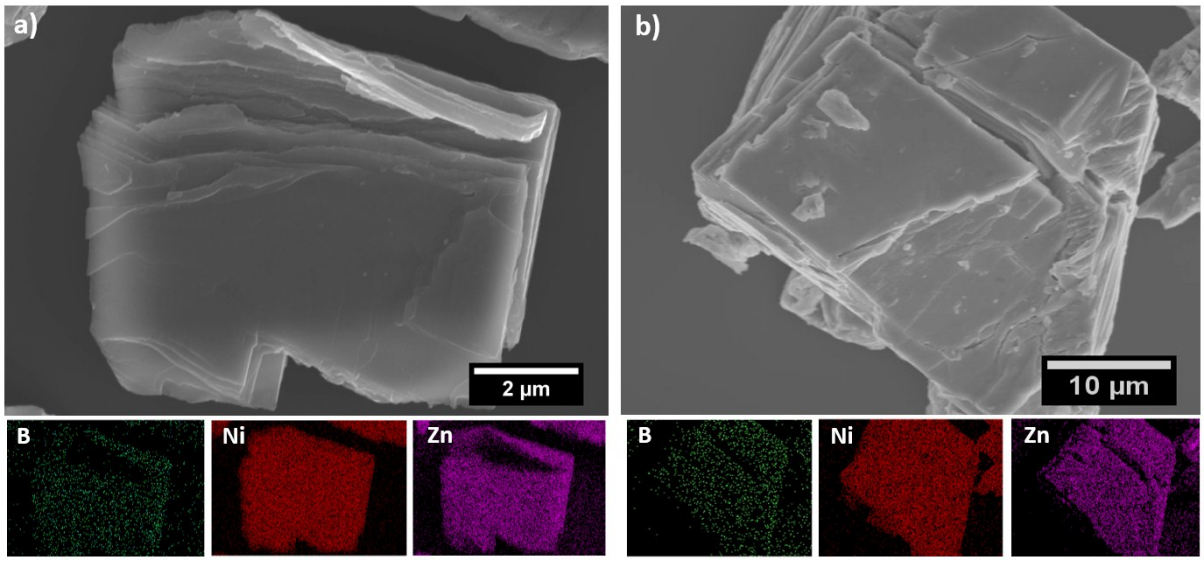

Figure S5. SEM image and EDS Analysis of as synthesized and un-etched (a) Ni_2ZnB and (b) Ni_3ZnB_2.

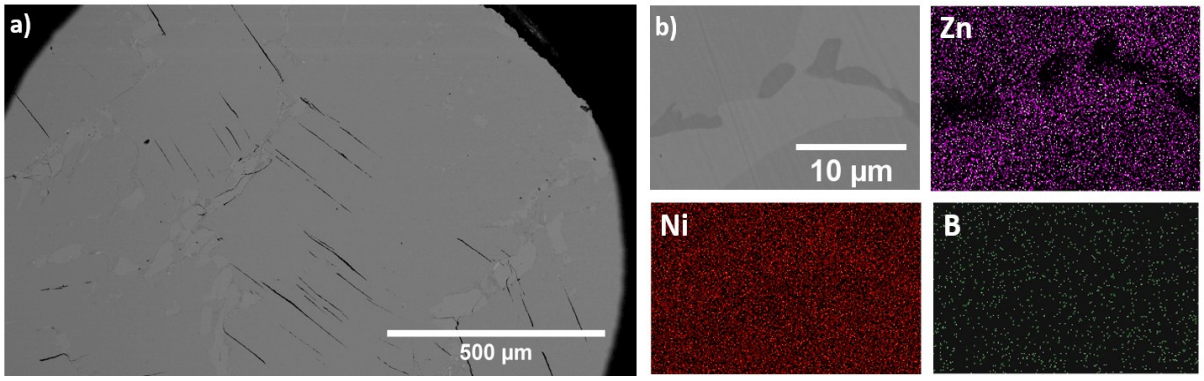

Figure S6. Backscattering SEM image of (a) as synthesized Ni_2ZnB button and (b) an enlarged part showing Ni-rich inclusions as proved by EDS Analysis.

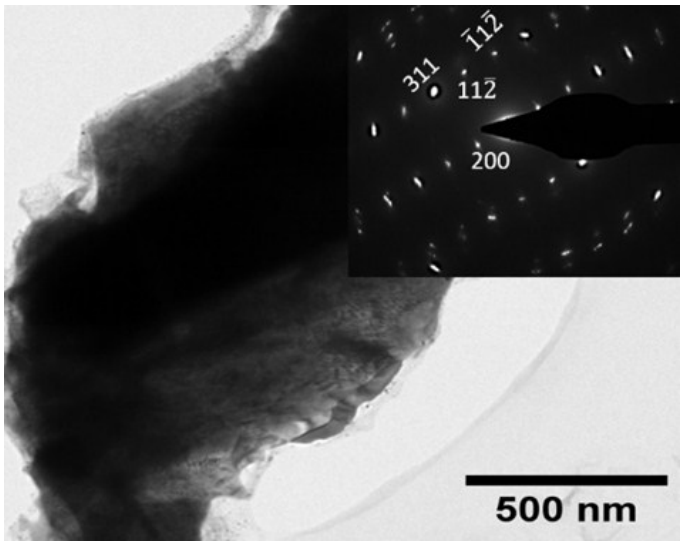

Figure S7. TEM image of a sonicated Ni_3ZnB_2 crystal and its selected area diffraction showing diffraction spots corresponding to the Ni_3ZnB_2 crystal structure (space group *C*2/*m*).

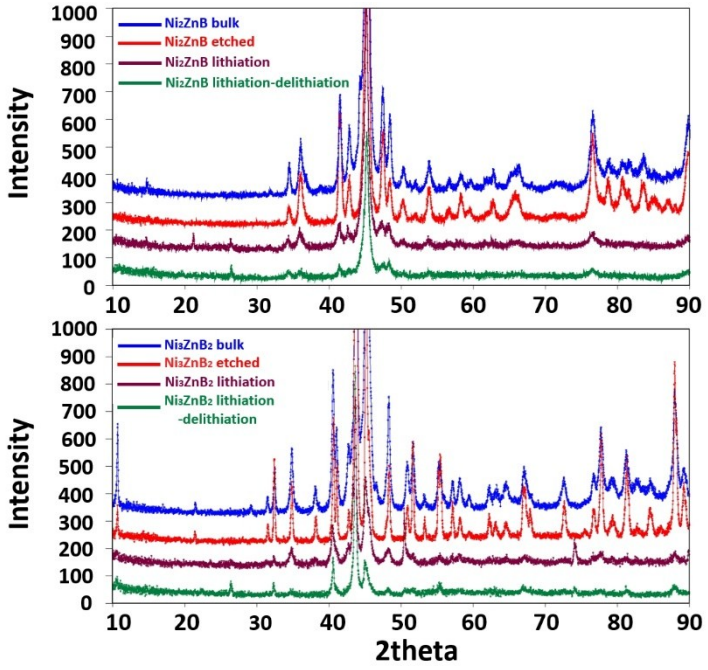

Figure S8. Magnified **p**owder XRD patterns of (a) Ni_2ZnB and (b) Ni_3ZnB_2 before etching (blue), after etching (red), after lithiation (magenta) and lithiation-delithiation (green) cycle.

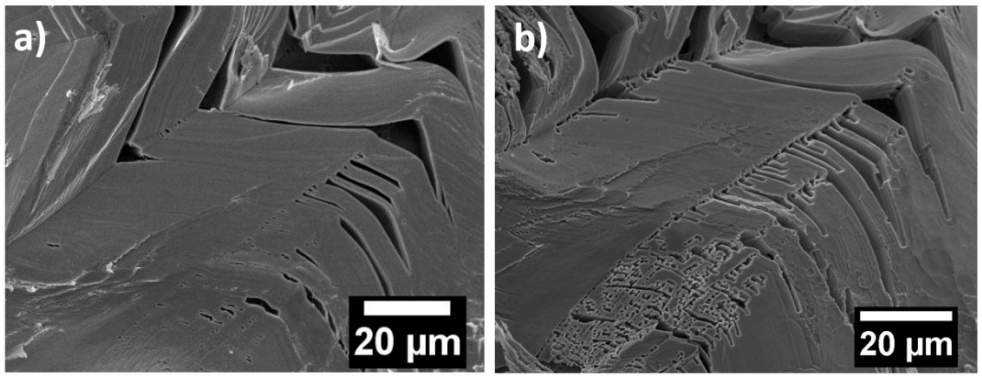

Figure S9. SEM images of an (a) unetched and (b) a 5-hr etched surface of Ni_2ZnB, showing pore formation upon etching.

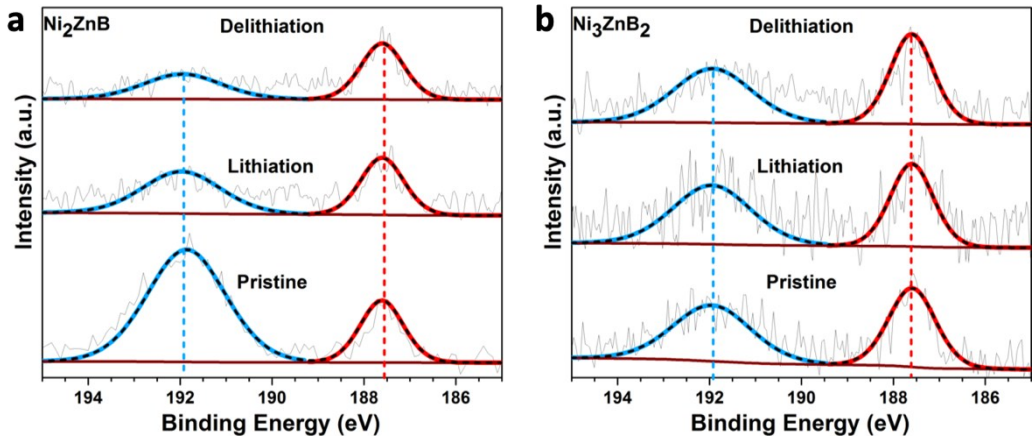

Figure S10. XPS B 1s spectra of (a) Ni_2ZnB and (b) Ni_3ZnB_2 at the pristine state and after lithiation and delithiation.

References:

1. Park H, Encinas A, Scheifers JP, Zhang Y, Fokwa BP. Boron‐Dependency of Molybdenum Boride Electrocatalysts for the Hydrogen Evolution Reaction. Angewandte Chemie International Edition. 2017;56(20):5575-8.
2. Naguib M, Kurtoglu M, Presser V, Lu J, Niu J, Heon M, et al. Two‐dimensional nanocrystals produced by exfoliation of Ti3AlC2. Adv Mater. 2011;23(37):4248-53.
3. Ghidiu M, Lukatskaya MR, Zhao M-Q, Gogotsi Y, Barsoum MW. Conductive two-dimensional titanium carbide 'clay'with high volumetric capacitance. Nature. 2014;516(7529):78.
4. Li M, Lu J, Luo K, Li Y, Chang K, Chen K, et al. Element Replacement Approach by Reaction with Lewis Acidic Molten Salts to Synthesize Nanolaminated MAX Phases and MXenes. Journal of the American Chemical Society. 2019;141(11):4730-7.
5. Rodriguez-Carvajal J. FullProf 2000: A Rietveld refinement and pattern matching analysis program. Version: April. 2008.
6. Failamani F, Podloucky R, Bursik J, Rogl G, Michor H, Müller H, et al. Boron-phil and boron-phob structure units in novel borides Ni3Zn2B and Ni2ZnB: experiment and first principles calculations. Dalton Transactions. 2018;47(10):3303-20.